ACS Catalysis

Open Access
This article is licensed under CC-BY 4.0

pubs.acs.org/acscatalysis
Research Article

Discovering Enantioselective Protodeauration in Gold Catalysis: Asymmetric Synthesis of Cyclobutenes

Yuhao Huang, Riccardo Giovanelli, Sofia Kiriakidi, Andrea Mazzanti, Carlos Silva López,* Giulio Bertuzzi,* and Marco Bandini*

Cite This: *ACS Catal.* 2026, 16, 10721−10729
Read Online

ACCESS | Metrics & More | Article Recommendations | Supporting Information

ABSTRACT: The accessibility to highly enantiomerically enriched organic compounds via asymmetric gold catalysis has grown exponentially for the past two decades. In the present study, we disclose the possibility to conduct asymmetric gold transformations exploiting asymmetric protodeauration events that are generally assumed as "innocent" elementary steps from a stereoselective viewpoint. As a proof of concept, we hereby report the synthesis of densely functionalized cyclobutenes (yields up to 82%), featuring an all-carbon quaternary stereogenic center, via a gold-catalyzed chemo-, regio-, and enantioselective (*ee* up to 96%) desymmetrization of bicyclo[1.1.0]butanes with allenamides. The "chelating" activation mode exerted by the binuclear chiral gold complex was ascertained by dedicated DFT calculations, while a deep understanding of the key role played by the protodeauration (genuine intramolecular profile, stereochemistry rationalization) was achieved via combined experimental and theoretical investigations.

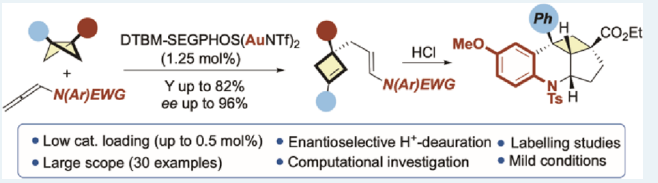

KEYWORDS: *enantioselective synthesis, protodeauration, gold catalysis, allenamides, bicyclobutanes*

INTRODUCTION

Enantioselective gold catalysis has rapidly reached a prominent role in asymmetric organic synthesis leading to the discovery of unprecedented stereoselective manipulations of unsaturated hydrocarbons via both C−C and C−X bond-forming reactions.[1−4] The reason behind this popularity can be found in the availability of a large portfolio of dedicated chiral ligands/counterions,[5−14] as well as in the adaptability of asymmetric gold transformations to enabling technologies and straightforward applications in total synthesis.[15−21] Additionally, convenient access to mechanistic rationales via combined spectroscopic and computational analyses further strengthened this scenario with a solid predictive profile.[22−27]

The unique peculiarity of asymmetric gold catalysis is the wealth of chemical species readily accessible, despite gold-mediated reaction machineries consisting of quite a narrow number of elementary steps. As a matter of fact, most enantioselective transformations based on cationic chiral gold complexes face an initial enantio-discriminating addition of a nucleophilic partner to the Au-activated unsaturated hydrocarbon. This event commonly culminates with the formation of reactive organogold intermediates, terminating the catalytic cycle via electrophilic/nucleophilic quenching or protodeauration steps (Figure 1).[28] In this scenario, the overall enantiocontrol of the process is generally exerted at the initial stage of the catalytic cycle with the final events featuring a mere bystander role from the perspective of asymmetric discrimination.

This is particularly relevant in the case of terminal protodeauration steps that, being quite often downhill in energy and involving solvent/strong acid-mediated proton sources (*i.e.*, MsOH, TfOH, AcOH), have never been targeted as a plausible stereodiscriminating chemical tool in gold catalysis.[29−35] As a consequence, providing solid solutions to this open challenge would contribute to significantly expand the chiral chemical spaces accessible via gold catalysis by allowing both steps of the catalytic cycle to be targeted toward new enantioselective approaches.

Within our research frameworks dedicated to the development of asymmetric gold-catalyzed protocols[36−46] and discovery of new efficient ligands for homogenous Au(I) catalysis,[47,48] we recently documented the effective [Au^+]-mediated dual activation of bicyclo[1.1.0]butanes (BCBs) **1** toward highly efficient [2π+2σ] cycloaddition with allenamides **2** (Scheme 1, top).[49] Here, the initial α-alkylation of the BCB leads to alkenyl-gold intermediate **D** that completes the [2+2] cycloaddition pathway via C−C bond-forming ring closure (**B** → **3'**). However, we speculated that the reaction machinery could be terminated differently if a protodeauration quench of the alkenyl-Au adduct **B**

Received: March 25, 2026
Revised: May 8, 2026
Accepted: May 11, 2026
Published: May 22, 2026

ACS Publications
© 2026 The Authors. Published by American Chemical Society

https://doi.org/10.1021/acscatal.6c02231
ACS Catal. 2026, 16, 10721−10729

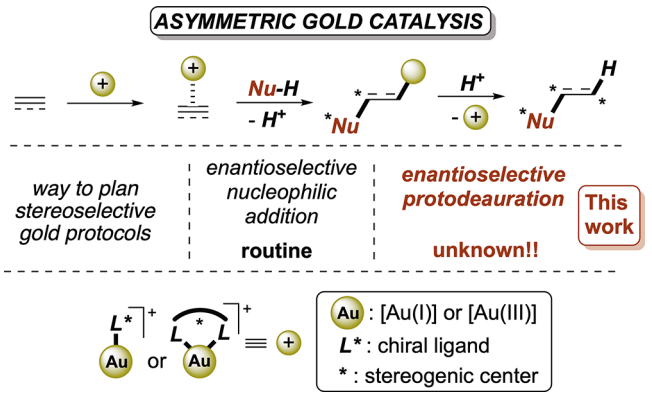

Figure 1. Elementary steps for a typical gold-catalyzed enantioselective transformation. The final protodeauration event still remains elusive from the control of the stereochemical profile.

precludes the ring-closing event, leading to densely functionalized cyclobutenes **3**.[50−52] Interestingly, compound **3** would present an all-carbon quaternary stereogenic center with the absolute configuration fully governed by the final protodeauration step of intermediate **B** (*i.e.*, discrimination of enantiotopic methylene groups). This hypothesis prompted us to the challenge of a stereoselective formation of cyclobutenes **3** via an unprecedented desymmetrization of bicyclo[1.1.0]butanes involving a final enantioselective protodeauration step. It is interesting to note that, although several enantioselective desymmetrization reactions have been documented under gold catalysis, their enantiodiscriminating events always rely on initial C−C as well as C−X bond-forming steps;[53−58] contrarily, enantioselective protodeauration steps are unprecedented so far.

■ RESULTS AND DISCUSSION

To test our working hypothesis, we envisioned taking advantage of the dual gold activation[59−61] recently discovered by us in the [2+2] cycloaddition.[49] In particular, we speculated that implementing this activation mode via binuclear chiral gold complexes (**C**) could lead to a conformationally rigid alkenyl-gold species **D**, providing the stereochemically discriminating environment needed for the subsequent proton transfer (Scheme 1, bottom).

Scheme 1. Previous Findings on Gold-Catalyzed Activation of BCBs (Top) Led to the Present Working Hypothesis: Probing Feasibility on Enantioselective Gold Catalysis Based on Stereoselective Protodeauration (Bottom)

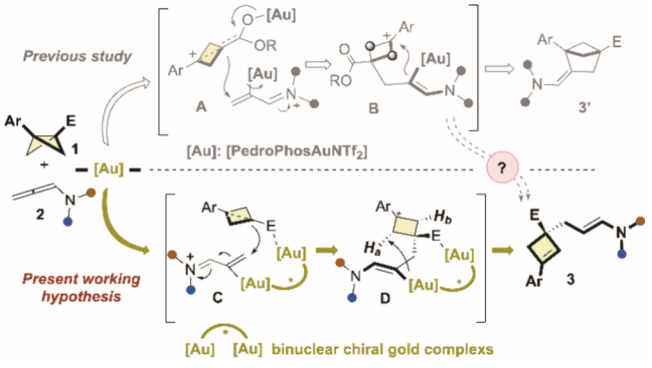

In addition, based on our previous findings on the stereoselective dearomatization of indoles with cumulenes,[62−65] we hypothesized that the use of *N*-sulfonyl-allenamides **2** should favor the protodeauration event toward the cycloaddition pathway.

Thus, a range of pre-formed and structurally rigid binuclear gold complexes (**Cat1−6**) were tested in the model C−C bond activation procedure involving bicyclo[1.1.0]butane **1a** and *N*(Ph)Ts-allenamide **2a** (Table 1). Here, we surveyed a large portfolio of reaction parameters (*i.e.*, solvent, stoichiometry, reaction media, catalyst loading). Satisfyingly, optimal conditions were conveniently distilled with binuclear [(*R*)-DTBM-SEGPHOS(AuNTf$_2$)$_2$] as the catalyst (1.25 mol %) that delivered the desired cyclobutene (*R*)-**3aa** as the major compound (**3aa**:**3aa'** = 7:1) in 78% isolated yield and 94% enantiomeric excess (entry 1, Table 1).

Interestingly, the **3** *vs* **3'** chemoselectivity proved to be strictly connected to the molecular skeleton of the ligand. As a matter of fact, by diminishing the steric hindrance of the *P*-substituents (*i.e.*, xylyl in **Cat2** and phenyl in **Cat3**), the [2+2]-cycloadduct **3'** became predominant with a concomitant drop in the enantiocontrol on cyclobutene **3** (94% → 25% *ee*). Similarly, the chemoselectivity of the reaction profile was deeply affected by the backbone of the chiral ligand. Here, MeO-BIPHEP-based catalysts **Cat4**/**5** or the binaphthyl-based complex **Cat6** led to the formation of the [2+2]-cycloadduct **3'** predominantly (entries 4 and 5) or extensive decomposition

Table 1. Optimization of Reaction Conditions[a]

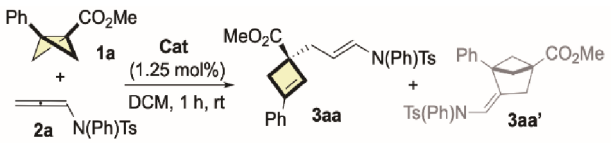

Cat1: (*R*)-DTBM-SEGPHOS(AuNTf)$_2$ **Cat4**: (*S*)-DTBM-MeO-BIPHEP(AuNTf)$_2$
Cat2: (*R*)-Xylyl-SEGPHOS(AuNTf)$_2$ **Cat5**: (*S*)-Xylyl-MeO-BIPHEP(AuNTf)$_2$
Cat3: (*R*)-SEGPHOS(AuNTf)$_2$ **Cat6**: (*S*)-BINAP(AuNTf)$_2$

entry	cat/cond.	3aa:3aa'[b]	yield (%) 3aa or 3aa'[c]	*ee* (%) 3aa[d]
1	**Cat1**/-	7:1	78 (3)	94
2	**Cat2**/-	1:1	34 (3)	86
3	**Cat3**/-	1:3.3	16 (3)	25
4	**Cat4**/-	1:1.3	27 (3)	−94
5	**Cat5**/-	1:1.3	28 (3)	−84
6	**Cat6**/-		21 (3')	
7[e]	**Cat1**(SbF$_6$)$_2$/-	2.4:1	67	84
8[e]	**Cat1**(TFA)$_2$/-		NR	
9	**Cat1**/ACN		20 (3')	
10	**Cat1**/toluene	2:1	60 (3)	95
11	**Cat1**/THF	1.2:1	36 (3)	70
12[f]	**Cat1**/-	5:1	56 (3)	94
13[g]	**Cat1**/-	6.7:1	76 (3)	92

[a]All reactions were carried out as depicted in the scheme of Table 1 under nitrogen conditions in the dark (**1a**:**2a** = 1:1.5, [**1a**] = 0.10 M), unless otherwise mentioned. All complexes **Cat1−6** were pre-formed. NR: no reaction. [b]Determined via crude ^{1}H-NMR with CH_2Br_2 as an internal standard. [c]Isolated yield after flash chromatography. [d]Determined via chiral stationary phase HPLC. The absolute configuration of compound **3aa** was assigned by analogy to compound **4ag** (see Scheme 3 and SI for details). [e]The activation of the complexes was performed *in situ* with the corresponding silver salts. [f]The reaction was carried out with a 1:1 ratio (**1a**:**2a**). [g]mmol scale reaction ([**1a**] = 0.20 M) **Cat1**: 0.5 mol %.

https://doi.org/10.1021/acscatal.6c02231
ACS Catal. 2026, 16, 10721−10729

of the starting materials (entry 6). Screenings of alternative gold counterions (*i.e.,* SbF_6 and TFA, entries 7 and 8, respectively) and reaction media (*i.e.* ACN, toluene, and THF, entries 9−11, respectively) provided less satisfactory chemical as well as stereochemical outcomes. Finally, optimal conditions were successfully implemented into a mmol scale variant (entry 13). Here, no significant erosion on both chemo- (**3aa**:**3aa'** = 6.7:1) and enantioselectivity (92% *ee*) was recorded in the presence of 0.5 mol % **Cat1**.

Then, our attention moved to the assessment of the robustness of the protocol. With this goal in mind, a range of diversely substituted allenamides (**1b−k**) were reacted with BCB **1a** (Scheme 2a). The importance of the EWG on the nitrogen atom was first investigated. Both sulfonyl groups different from tosyl, such as methanesulfonyl (*i.e.* Ms, **2b**) and 2-nitrobenzenesulfonyl, as well as carbamoyl protecting units, like Cbz and Moc, performed satisfyingly, by guaranteeing a level of enantioselection up to 95% (**3ae**). Then, we focused on the generality of the *N*-Ar segment of the allenyl compound. Here, allenamides **2f−k** were reacted by accommodating both EWGs and EDGs at different positions of the phenyl ring. Remarkably, the methodology featured excellent robustness in all cases, providing the corresponding cyclobutenes **3af−3ak** with a stereochemical control as high as 96% *ee*.

The modulability of the Cα-ester was initially assessed by using BCBs **1b−d** bearing benzyl, ethyl, and allyl, esters respectively. In these cases, the desymmetrization protocol worked smoothly, resulting in cyclobutenes **3ba−3da** in up to 82% yield and excellent enantioselectivity (87−94% *ee*). Esters were then replaced by a range of aliphatic and aromatic ketones (**1e−i**). Isolated yields were generally slightly lower than those of ester analogous (up to 46%). Importantly, in these cases, a solvent switch from DCM to toluene was pivotal to impart a synthetically useful level of stereoselection (60−84% *ee*, see Supporting Information for details). Finally, a comprehensive decoration of BCBs **1** was achieved by installing both EWGs and EDGs on the aryl ring at the Cγ position. In particular, halides (**1j−l** and **1r**), alkyl (**1m−p** and **1p,q**), and methoxy (**1o**) substituents were accommodated delivering, in all cases, appreciable yields and high enantioselectivities. Only in the case of *ortho*-substituted phenyl rings **1q** and **1r** a slightly lower efficiency was recorded (yield: 32−51%). However, the enantioselection was unaffected (86−88% *ee*). Finally, the protocol was proven to tolerate π-extended rings as well (*i.e.,* naphthyl, **1s**), resulting in the corresponding cyclobutene **3sa** in 57% isolated yield and 94% enantiomeric excess. Delightfully, the protocol proved its effectiveness also in the case of BCB **1t** carrying an aliphatic substituent at the Cγ position (*i.e.,* $-(CH_2)_2Ph$), delivering the corresponding cyclobutene **3ta** in good enantiomeric excess (81% *ee*).

The high density of functional groups in the enantio-enriched cyclobutenyl scaffolds prompted us to investigate their chemical

Scheme 2. Generality of the Protocol: (a) Versatility toward Allenamides; (b) Variations on the Cα-Electron-Withdrawing Group on 1; (c) Variations on the Cγ-Substituent Ring on 1[a]

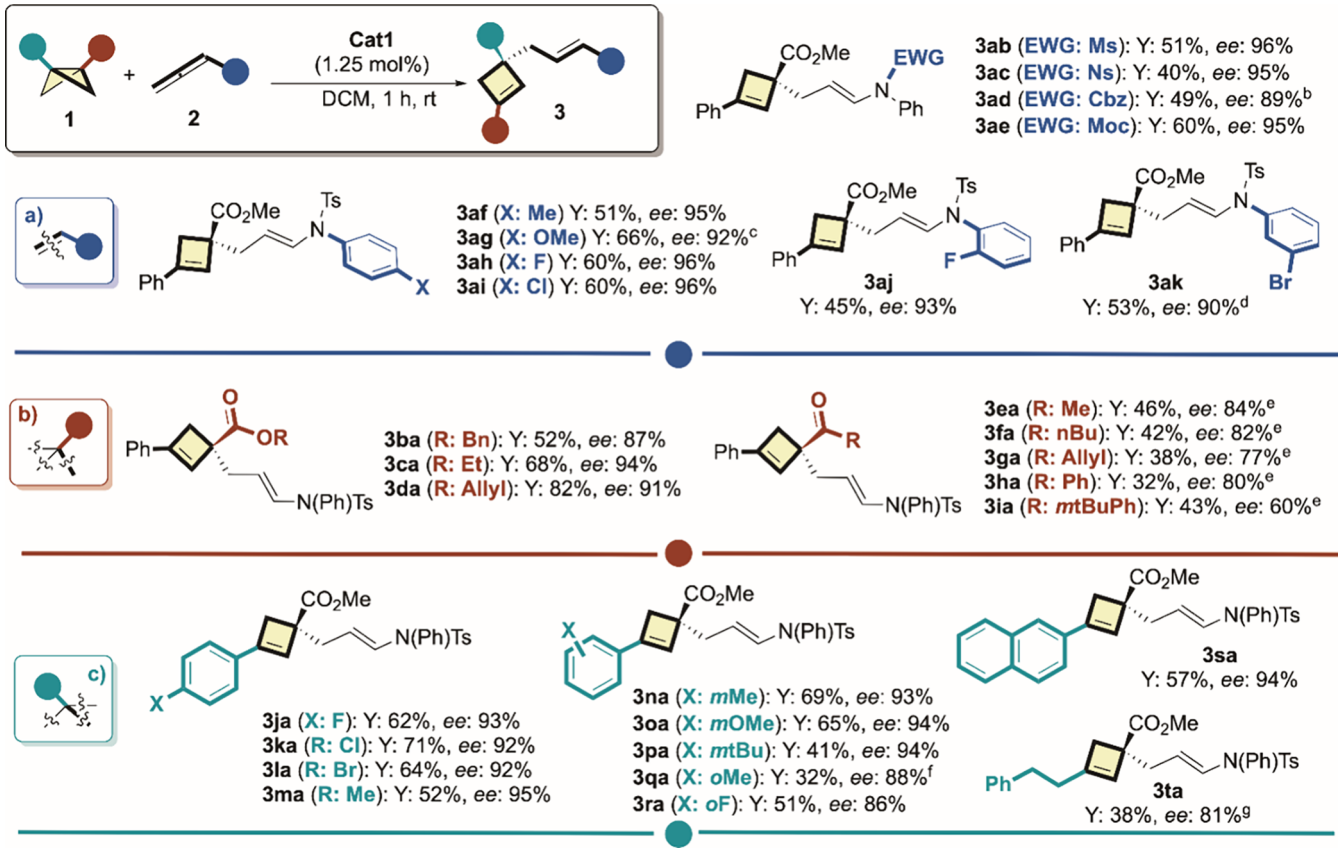

[a]Experimental details on the reaction parameters can be found in the Supporting Information. All compounds were isolated with an *E*:*Z*-ratio of the C=C > 20:1. [b]With 2.5 mol % **Cat1** and 72 h. [c]With 2.5 mol % **Cat1**. [d]With 0.5 mol % **Cat1**. [e]In toluene. [f]72 h reaction time. [g]With 3.75 mol % **Cat1** and 2 h reaction time.

https://doi.org/10.1021/acscatal.6c02231
ACS Catal. 2026, 16, 10721−10729

Scheme 3. Chemical Elaboration of Cyclobutene 3ag (E = CO_2Et)

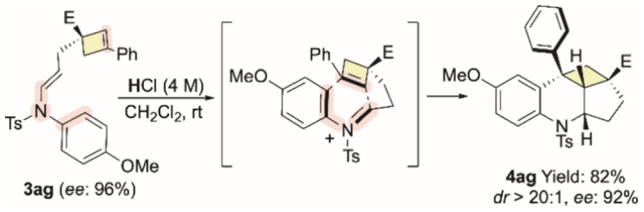

versatility. Interestingly, when **3ag** was treated with HCl (4 M in 1,4-dioxane), a complex skeletal rearrangement was observed, delivering the tetracyclic fused compound **4ag** (82% yield) via a Povarov-like cyclization.[66−69] In this transformation, four consecutive stereogenic centers were allocated at the rigid scaffold in excellent diastereoselectivity and complete retention of the starting enantiomeric excess (*dr* > 20:1, *ee* 92%, Scheme 3).

Thereafter, the mechanistic profile of the reaction was investigated. In this regard, a nonlinear effect (NLE) study was carried out to support the postulated templating effect imprinted by the binuclear gold complex on the stereoselective protodeauration step (Figure 2A).[70,71]

Herein, the linear behavior observed plotting the *ee* (%) of product **3aa** versus the *ee* (%) of **Cat1** supports the involvement of a single molecule of the binuclear catalyst in the enantiodiscriminating event. This, together with the previously disclosed dual-activation profile of the [2σ+2π] cycloaddition, where a mono-nuclear Au-catalyst was employed, supports the hypothesis of the engagement of both gold atoms of **Cat1** in the stereodetermining step (*vide infra* for supporting computational studies). Furthermore, to get more insights into the prominence of the protodeauration step, an extensive labeling investigation was carried out (Figure 2B). To this aim, previously unreported deuterated BCB ***d*⁴-1a** was conveniently synthetized (see Supporting Information for details) and subjected to optimal reaction conditions (Table 1, entry 1). Interestingly, cyclobutene ***d*⁴-3aa** was isolated in 65% yield and 91% enantiomeric excess. Most importantly, full deuteration (95%) of the electron-rich carbon of the enamide sidearm was observed (Figure 2Ba).

Further insights on the protodeauration step were obtained through a crossover control experiment (Figure 2Bb). Specifically, by employing an equimolar mixture of BCBs **1n** and ***d*⁴-1a** in the model reaction with allenamide **2a**, two products (**3na** and ***d*⁴-3aa**) were formed (56% overall yield) without any detectable crossover contamination (*i.e.*, **D** and H scrambling) during the final stage of the enantioselective machinery. This observation unambiguously supports the intramolecular nature of the final protodeauration. Subsequently, a kinetic isotopic effect experiment[72] was conducted using an equimolar mixture of ***d*⁴-1a** and **1a** as the starting material (**1**:**2a** = 5:1, Figure 2Bc). Interestingly, compounds ***d*⁴-3aa** and **3aa** were isolated in 59% overall yield and 1.7:1 ratio favoring the non-deuterated isomer. These results suggest that the protodeauration, although serving as the stereodetermining step, likely does not impact greatly the kinetics of the enantioselective gold-catalyzed allylation protocol.

Once the main mechanistic features of the reaction were addressed from an experimental view point, we resorted to computational simulations to gain an atomistic perspective of the catalytic process. B97-3c as implemented in Orca,[73,74] a highly efficient and robust composite electronic structure method developed with thermochemistry, geometries, and non-covalent interactions in mind, was used to be able to maintain fully quantum simulations despite the significant challenges that this chemistry poses. The machinery under scrutiny is particularly difficult to simulate since

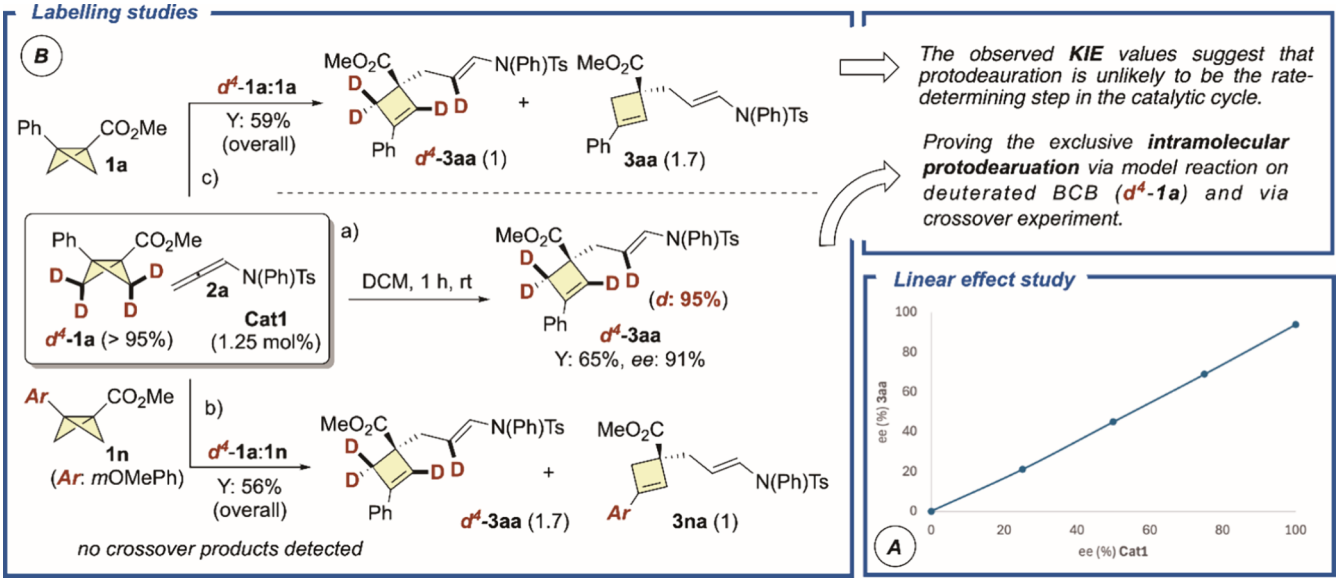

Figure 2. Experimental investigations toward the definition of the reaction machinery. (A) Linear effect study carried out on the **1a** + **2a** model reaction (**Cat1** = 1.25 mol %, CH_2Cl_2, rt, 1 h). (B) Labeling experiments: (a) proving the involvement of the methylene units of the cyclobutyl group in the protodeauration step of the reaction; (b) the crossover experiment excludes an intermolecular proton-exchange phenomena during the protodeauration; (c) a small kinetic isotope effect suggests that the protodeauration is hardly kinetically relevant in the catalytic cycle. Experimental details for the labeling studies: (a) ***d*⁴-1a**:**2a** (1:1.5), ***d*⁴-1a** = 0.10 mM; (b) **Cat1** = 1.25 mol %, ***d*⁴-1a**:**1n** (1:1), **1**:**2a** (3:1), **2a** = 0.10 M, CH_2Cl_2, rt, 1 h; (c) **Cat1** = 1.25 mol %, ***d*⁴-1a**:**1a** (1:1), **1**:**2a** (5:1), **2a** = 0.05 M, CH_2Cl_2, rt, 1 h. Deuterium incorporation was determined by ^{1}H-NMR on the reaction crudes.

https://doi.org/10.1021/acscatal.6c02231
ACS Catal. 2026, 16, 10721−10729

stereoselectivity requires very accurate energy values but the sheer size of the catalyst prevents the use of most first-principles models. Due to the proven sensitivity of this chemistry with respect to structural modifications both on the substrate and the catalyst, we decided to be very conservative in terms of truncations. In particular, the reaction was simulated by assuming the best performing bicationic complex [**Cat1**]$^{2+}$ with only two *tert*-butyl groups simplified as methyl substituents (only those located far and oriented away from the reacting substrates). A slight truncation of allenamide **2a** into **2a**† featuring -*N*(Me)Ms instead of −*N*(Ph)Ts substituents was also performed.

Interestingly, two precomplex structures were found corresponding to the initial C−C bond-forming reaction (**Int1** and **Int1'**). In these precomplex structures, the geometry of the substrates seems already prearranged to favor the formation of either cyclobutene enantiomer (the BCB moiety exposes opposite faces, hence opposite hydrogen atoms, to the catalyst), showing significant stability difference between these two poses of the substrates on the catalyst (11.5 kcal/mol, favoring **Int1**, light blue pathway). Then, the C−C bond is formed through easily accessible transition states where the blue pathway is also favored, but by a smaller margin (2.4 kcal/mol). Once the first bond is formed, two stable coupled intermediates are found (**Int2** and **Int2'**). This is in striking contrast to previous findings with monodentate *PedroPhos*-based Au complex (Scheme 1 top). With such a catalyst, once the first C−C bond was formed, a subsequent barrierless collapse of a second C−C bond yielded bicyclic structures **3'**.[49] In this case, however, the steric contacts of the bulky bidentate DTBM-SEGPHOS ligand and the intrinsic lower nucleophilic properties of σ-alkenyl-Au intermediates **Int2** deriving from *N*-sulfonyl-allenamides with respect to oxazolidinyl ones, together with the stabilizing effect of the phenyl substituent of BCB on the carbocationic structure, allow for this key intermediate to become stable. Actually, not only intermediates **Int2** and **Int2'** become stable, but the otherwise barrierless collapse to form the second C−C bond here becomes the less competitive process (**TS3**, black pathway) by about 6 kcal/mol compared to the two alternative hydrogen shifts yielding cyclobutenes **3** (**TS2** and **TS2'**). In agreement with the experimental findings, the protodeauration is not found to be rate limiting, but it is also not an innocent and barrierless step as has often suggested to be in gold chemistry.

Scheme 4. General Features of the Reaction Profile[a]

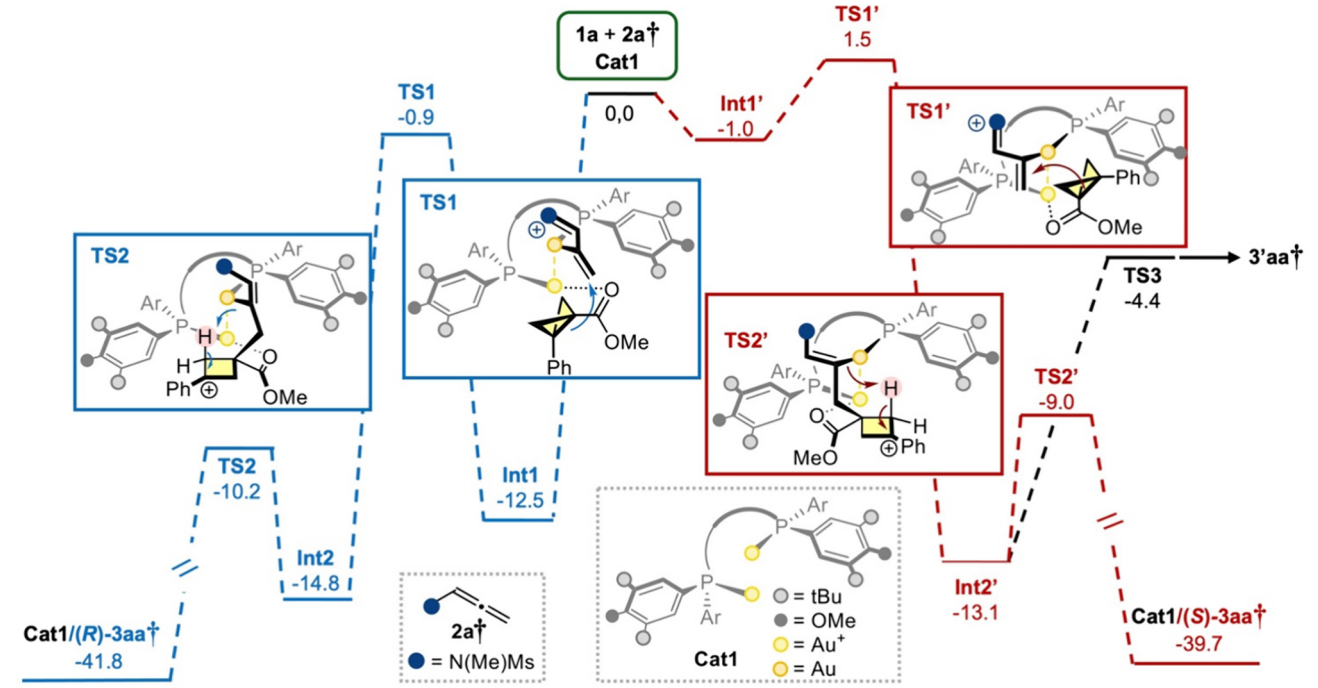

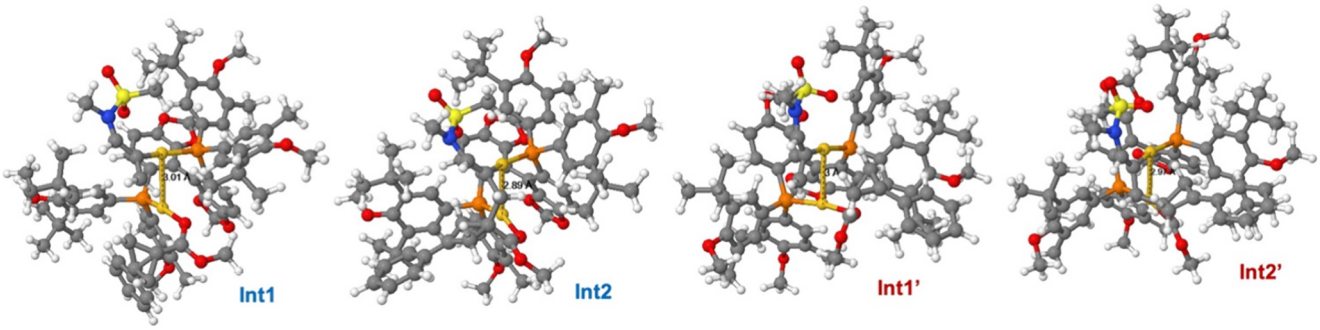

[a]Values shown are relative Gibbs free energies computed at 298 K and 1 atm.

https://doi.org/10.1021/acscatal.6c02231
ACS Catal. 2026, 16, 10721−10729

Notably, the calculations also substantiated the initial hypothesis of a dual gold activation mode exerted by the binuclear **Cat1**. Here, the simultaneous coordination of both allenamide (π-acidity) and BCB (σ-acidity) by the two gold atoms leads to a desired proximity effect of the reaction partners and dictate a rigid and desirable mutual orientation for the initial C−C bond-forming reaction. Additionally, this initial orientation (**Int1** and **Int1'**) seems to determine the final geometry of the eventually formed cyclobutene. Careful inspection of these two structures reveals that the phenyl substituent of the BCB fragment clashes with *t*-butyl groups in **Int1'** whereas, in **Int1**, it rests well accommodated in a perpendicular orientation with respect to the P-C(Ph) bond such that it avoids most of the steric contacts with the bulky alkyl substituents (see Supporting Information). This situation is partially propagated in the entire path up to the transition states associated to the proton migration. In them, in order to avoid the mentioned destabilizing steric contacts, the reactant adopts a less efficient bidentate pose for **TS2'**, with strained biting angles, particularly for the carbonyl ligand (the AuOC angle is 129° in **TS2'**, whereas **TS2** shows a more natural value of 125°, which implies a more aptly directed lone pair from the carbonyl oxygen toward the gold center). This is also reflected in the Au−Au distances (2.91 Å in **TS2** *vs* 2.98 A in **TS2'**).

Additionally, due to the tight fit of the substrates in the catalyst, it would not be possible to obtain (*S*)-**3aa**† from **Int1**, and conversely (*R*)-**3aa**† is not accessible from **Int1'** without paying a large energy penalty (see the Supporting Information for further details). The lowest energy path for this to happen would involve decomplexation of the ligands and re-complexation in the alternative pose. In summary, calculations match the stereoinduction observed in the catalytic protocol, emphasizing the pathway leading to the *R*-stereoisomer as the most likely one.

■ CONCLUSIONS

In conclusion, a new paradigm in enantioselective gold catalysis has been proposed and successfully demonstrated. The stereoselective protodeauration step was exploited to access enantiomerically enriched cyclobutenes (up to 96% *ee*) through the site-selective desymmetrization of densely functionalized bicyclo[1.1.0]butanes. The formation of an all-carbon quaternary stereogenic center was efficiently achieved via electrophilic activation of allenamides using chiral gold complexes. The high efficiency of the catalytic system is highlighted by the low catalyst loading required (down to 0.5 mol %) while maintaining excellent chemical yields and stereochemical outcomes. A detailed mechanistic investigation, combining isotopic labeling experiments, nonlinear effect analysis, and DFT calculations, unambiguously identified the intramolecular modality of the protodeauration event and provided a rationale for the observed chemical as well as stereochemical outcomes. Efforts to extend the concept of protodeauration-mediated enantioselective gold catalysis to other reaction manifolds are currently underway in our laboratories and will be reported in due course.

■ METHODS

General Procedure for the Preparation of Enantio-enriched Products 3

In a heat-gun dried 10 mL two-necked round bottomed flask covered with an aluminium foil, under an inert atmosphere (Ar), the appropriate bicyclo[1.1.0]butane **1** (0.1 mmol, 1 equiv), the appropriate allenamide **2** (0.15 mmol, 1.5 equiv), and **Cat1** (0.00125 mmol, 2.7 mg, 1.25 mol %) were stirred in dry DCM (1.0 mL) at room temperature in the dark for 1 h. The solvent was then evaporated, and the crude mixture was directly purified by FC on silica gel.

Note: The reactions leading to products **3ea**, **3fa**, **3ga**, **3ha**, and **3ia** were run in toluene for 16 h instead of DCM for 1 h. In these cases, an increase in the enantiomeric excess was observed by switching solvent, although accompanied by a slower reaction.

Preparation of Compound 4ag

In a flame-dried small round bottom flask, compound **3ag** (50.3 mg, 0.1 mmol) was dissolved in dry DCM (0.5 mL) and HCl (4 M in dioxane, 0.1 mL, 0.4 mmol) was added. The resulting mixture was stirred at room temperature for 3 h, after which it was directly purified by FC on silica gel to afford pure product **4ag**.

■ ASSOCIATED CONTENT

Data Availability Statement

Input and output files for all the structures in are available at the ioChem-DB: https://doi.org/10.19061/iochem-bd-6-634

Supporting Information

The Supporting Information is available free of charge at https://pubs.acs.org/doi/10.1021/acscatal.6c02231.

Experimental procedures for the catalytic protocols and for the control experiments directed to the reaction mechanism elucidation; analytical characterization of the new chemical compounds (DOCX)

■ AUTHOR INFORMATION

Corresponding Authors

Carlos Silva López – *Departamento de Química Orgánica, Universidade de Vigo, AS Lagoas (Marcosende) s/n, Vigo 36310, Spain;* orcid.org/0000-0003-4955-9844; Email: carlos.silva@uvigo.es

Giulio Bertuzzi – *Dipartimento di Chimica "Giacomo Ciamician", Alma Mater Studiorum, Università di Bologna, Via P. Gobetti 85, Bologna 40129, Italy; Center for Chemical Catalysis − C3 Alma Mater Studiorum, Università di Bologna, Via P. Gobetti 85, Bologna 40129, Italy;* Email: giulio.bertuzzi2@unibo.it

Marco Bandini – *Dipartimento di Chimica "Giacomo Ciamician", Alma Mater Studiorum, Università di Bologna, Via P. Gobetti 85, Bologna 40129, Italy; Center for Chemical Catalysis − C3 Alma Mater Studiorum, Università di Bologna, Via P. Gobetti 85, Bologna 40129, Italy;* orcid.org/0000-0001-9586-3295; Email: marco.bandini@unibo.it

Authors

Yuhao Huang – *Dipartimento di Chimica "Giacomo Ciamician", Alma Mater Studiorum, Università di Bologna, Via P. Gobetti 85, Bologna 40129, Italy; Center for Chemical Catalysis − C3 Alma Mater Studiorum, Università di Bologna, Via P. Gobetti 85, Bologna 40129, Italy*

Riccardo Giovanelli – *Dipartimento di Chimica "Giacomo Ciamician", Alma Mater Studiorum, Università di Bologna, Via P. Gobetti 85, Bologna 40129, Italy; Center for Chemical Catalysis − C3 Alma Mater Studiorum, Università di Bologna, Via P. Gobetti 85, Bologna 40129, Italy*

Sofia Kiriakidi – *Dipartimento di Chimica "Giacomo Ciamician", Alma Mater Studiorum, Università di Bologna,*

https://doi.org/10.1021/acscatal.6c02231
ACS Catal. 2026, 16, 10721−10729

Via P. Gobetti 85, Bologna 40129, Italy; Center for Chemical Catalysis − C3 Alma Mater Studiorum, Università di Bologna, Via P. Gobetti 85, Bologna 40129, Italy

Andrea Mazzanti − *Center for Chemical Catalysis − C3 Alma Mater Studiorum, Università di Bologna, Via P. Gobetti 85, Bologna 40129, Italy; Dipartimento di Chimica Industriale "Toso Montanari", Alma Mater Studiorum, Università di Bologna, Via P. Gobetti 85, Bologna 40129, Italy*

Complete contact information is available at: https://pubs.acs.org/doi/10.1021/acscatal.6c02231

Author Contributions

All authors have given approval to the final version of the manuscript.

Notes

The authors declare no competing financial interest.

■ ACKNOWLEDGMENTS

We are grateful to the University of Bologna for financial support and PRIN-2022-PNRR project (20227Z3BL8). M.B. is also grateful to Consorzio CINMPIS. Y.S. is grateful to CSC (grant no. 202408410138) for financial support. S.K. thanks the Xunta de Galicia for funding through the fellowship "Ayudas de apoyo a la etapa de formación posdoctoral (ED481B-2023-044)". C.S.L. is grateful the to the Centro de Supercomputación de Galicia for HPC resources and to MICINN (PID2020-115789GB-C22) for research funds.

Dedication

This work is dedicated to Professor Achille Umani-Ronchi on the occasion of his 90th birthday.

■ ABBREVIATIONS

BCB	bicyclo[1.1.0]butane
biphep	2,2'-bis(diphenylphosphino)-1,1'-biphenyl
Cbz	benzyloxycarbonyl
DCE	dichloroethane
DCM	dichloromethane
binap	2,2'-bis(diphenylphosphino)-1,1'-biphenyl
DTBM	3,5-di-*tert*-butyl-4-methoxyphenyl
EDGs	electron-donating groups
EWGs	electron-withdrawing groups
HPLC	high-pressure liquid chromatography
NMR	nuclear magnetic resonance
MS	methanesulfonyl
Ns	4-nitrobenzenesulfonyl
SEGPHOS	5,5′-bis(diphenylphosphino)-4,4′-bi-1,3-benzodioxole
OTF^-	trifluoromethanesulfonate
RDS	rate-determiningstep
SbF_6^-	hexafluoroantimonate
TFA	trifluoroacetate
TLC	thin-layer chromatography
xylyl	3,5-dimethylphenyl

■ REFERENCES

(1) Sengupta, S.; Shi, X. Recent Advances in Asymmetric Gold Catalysis. *ChemCatChem* **2010**, *2*, 609–619.
(2) Pradal, A.; Toullec, P. Y.; Michelet, V. Recent Developments in Asymmetric Catalysis in the Presence of Chiral Gold Complexes. *Synthesis* **2011**, *2011*, 1501–1514.
(3) López, F.; Mascareñas, J. L. Gold(I)-catalyzed Enantioselective Cycloaddition Reactions. *Beilstein J. Org. Chem.* **2013**, *9*, 2250–2264.
(4) Zi, W.; Toste, F. D. Recent Advances in Enantioselective Gold Catalysis. *Chem. Soc. Rev.* **2016**, *45*, 4567–4589.
(5) Loh, C. C. J.; Enders, D. Merging Organocatalysis and Gold Catalysis-A Critical Evaluation on the Underlying Concepts. *Chem. Eur. J.* **2012**, *18*, 10212–10225.
(6) Cera, G.; Bandini, M. Enantioselective Gold(I) Catalysis with Chiral Monodentate Ligands. *Isr. J. Chem.* **2013**, *53*, 848–855.
(7) Wang, Y. M.; Lackner, A. D.; Toste, F. D. Development of Catalysts and Ligands for Enantioselective Gold Catalysis. *Acc. Chem. Res.* **2014**, *47*, 889–901.
(8) Zuccarello, G.; Escofet, I.; Caniparoli, U.; Echavarren, A. M. New-Generation Ligand Design for the Gold-Catalyzed Asymmetric Activation of Alkynes. *ChemPlusChem* **2021**, *86*, 1283–1296.
(9) Jiang, J.-J.; Wong, M.-K. Recent Advances in the Development of Chiral Gold Complexes for Catalytic Asymmetric Catalysis. *Chem. Asian J.* **2021**, *16*, 364–377.
(10) Teixeira, P.; Bastin, S.; César, V. Fused Polycyclic NHC Ligands in Gold Catalysis: Recent Advances. *Isr. J. Chem.* **2022**, *63*, No. e202200051.
(11) Chintawar, C. C.; Patil, N. T. Enantioselective Redox Gold Catalysis. *Gold Bull.* **2022**, *55*, 161–168.
(12) Gade, A. B.; Urvashi; Patil, N. T. Asymmetric Gold Catalysis Enabled by Specially Designed Ligands. *Org. Chem. Front.* **2024**, *11*, 1858–1895.
(13) Pegu, C.; Paroi, B.; Patil, N. T. Enantioselective Merged Gold/organocatalysis. *Chem. Commun.* **2024**, *60*, 3607–3623.
(14) Patwa, A.; Pegu, C.; Paroi, B.; Patil, N. T. Enantioselective Gold/Enzyme Dual Catalysis. *Tetrahedron Lett.* **2025**, *154*, No. 155382.
(15) Hashmi, A. S. K.; Rudolph, M. Gold Catalysis in Total Synthesis. *Chem. Soc. Rev.* **2008**, *37*, 1766–1775.
(16) Pfästener, D.; Hashmi, A. S. K. Gold Catalysis in Total Synthesis − Recent Achievements. *Chem. Soc. Rev.* **2016**, *45*, 1331–1367.
(17) De, S.; Dan, A. K.; Sahu, R.; Parida, S.; Das, D. Total Synthesis of Natural Products Using Gold Catalysis. *Chem. − Asian J.* **2022**, *24*, No. e202200896.
(18) Lin, B.; Liu, T.; Luo, T. Gold-catalyzed Cyclization and Cycloaddition in Natural Product Synthesis. *Nat. Prod. Rep.* **2024**, *41*, 1091–1112.
(19) Mishra, S.; Urvashi; Patil, N. Y. Chiral Ligands for Au(I), Au(III), and Au(I)/Au(III) Redox Catalysis. *Isr. J. Chem.* **2023**, *63*, No. e202200039.
(20) Ambegave, S. B.; Shubham; More, T. R.; Patil, N. T. Gold-based Enantioselective Bimetallic Catalysis. *Chem. Commun.* **2023**, *59*, 8007–8016.
(21) Pegu, C.; Paroi, B.; Patil, N. T. Enantioselective Merged Gold/organocatalysis. *Chem. Commun.* **2024**, *60*, 3607–3623.
(22) Brown, T. J.; Weber, D.; Gagné, M. R.; Widenhoefer, R. A. Mechanistic Analysis of Gold(I)-Catalyzed Intramolecular Allene Hydroalkoxylation Reveals an Off-Cycle Bis(gold) Vinyl Species and Reversible C−O Bond Formation. *J. Am. Chem. Soc.* **2012**, *134*, 9134–9137.
(23) Obrados, C.; Echavarren, A. M. Intriguing Mechanisti Labyrinths in Gold(I) Catalysis. *Chem. Commun.* **2014**, *50*, 16–28.
(24) Faza, O. N.; López, C. S.; Slaughter, L. M. Computational Approaches to Homogenous Gold Catalysis, in Homogenous Gold Catalysis. *Top. Curr. Chem.* **2015**, *357*, 213–283.
(25) Daley, R. A.; Morrenzin, A. S.; Neufeldet, S. R.; Topczewski, J. J. Mechanistic Investigation into the Gold-catalyzed Decarboxylative Cross-coupling of Iodoarenes. *ACS Catal.* **2021**, *11*, 9578–9587.
(26) Segato, J.; Aneggi, E.; Baratta, W.; Campagnolo, F.; Belpassi, L.; Belanzoni, P.; Zuccaccia, D. Experimental and Theoretical Invesitgation of Ion Pairing in Gold(III) Catalysts. *Organometallics* **2023**, *42*, 2973–2982.

(27) Annibaletto, J.; Jacob, C.; Thilmany, P.; Loison, A.; Escorihuela, J.; Evano, G. Mechanistic Studies on the Gold-Catalyzed Intramoecular Hydroalkylation of Ynamides and Indenes. *ACS Omega* **2024**, *9*, 51690–51700.
(28) Mechanistically, although the protodeauration step can be arbitrarily considered an electrophilic quenching of organogold species, it is commonly distinguished by alternative E^+ + Au-C → E-C + Au+ steps resulting C-C or C-X structure finalizations.
(29) BabaAhmadi, R.; Ghanbari, P.; Rajabi, N. A.; Hashmi, A. S. K.; Yates, B. F.; Ariafard, A. A Theoretical Study on the Protodeauration Step of the Gold(I)-Catalyzed Organic Reactions. *Organometallics* **2015**, *34*, 3186–3195.
(30) Gaggioli, C. A.; Ciancaleoni, G.; Zuccaccia, D.; Bistoni, G.; Belpassi, L.; Tarantelli, F.; Belanzoni, P. Strong Electron-Donating Ligands Accelerate the Protodeauration Step in Gold(I)-Catalyzed Reactions: A Quantitative Understanding of the Ligand Effect. *Organometallics* **2016**, *35*, 2275–2285.
(31) Pérez-Iglesias, M.; Espinet, P.; Casares, J. A. Comparing Protonolysis and Transmetalation Reactions: Microcalorimetric Studies of C-Au(I) Bonds in [AuRL] Complexes. *Inorg. Chem.* **2018**, *57*, 11193–11200.
(32) Stylianakis, I.; Nieto Faza, O.; López, C. S.; Kolocouris, A. The Role of Protodeauration in the Gold-catalyzed Reaction of 1,3-Diynes with Pyrrole and Indole to form Complex Heterocycles. *Org. Chem. Front.* **2020**, *7*, 997–1005.
(33) Sciortino, G.; Muñoz-López, S.; Lledós, A.; Ujaque, G. Comparative Mechanistic Study on the $[Au(NHC)]^+$-Catalyzed Hydration of Alkynes, Alkenes, and Allenes. *Organometallics* **2020**, *39*, 3469–3479.
(34) Jo, T.; Taschinski, S.; Leach, I. F.; Bauer, C.; Hashmi, A. S. K.; Klein, J. E. M. N. On the Role of Noncovalent Ligand-Substrate Interactions in Au(I) Catalysis: An Experimental and Computational Study of Protodeauration. *ACS Catal.* **2022**, *12*, 13158–13163.
(35) Gallorini, G.; Kiriakidi, S.; Bellini, S.; López, C. S.; Bertuzzi, G.; Bandini, M. Site-Selective Gold-Catalyzed Alkylation of α-Aminotropones with Allenes. *Org. Lett.* **2024**, *26*, 9251–9256.
(36) Rivers, M.; Widenhoefer, R. A. Kinetis and Mechanism of the Protodeauration of Gold(I) β-Styrenyl Complexes. *Organometallics* **2025**, *44*, 1165–1175.
(37) Bandini, M.; Eichholzer, A. Enantioselective Gold-catalyzed Allylic Alkylation of Indoles with Alcohols: Efficient route to Functionalized Tetrahydrocarbazoles. *Angew. Chem., Int. Ed.* **2009**, *48*, 9533–9537.
(38) Bandini, M.; Monari, M.; Romaniello, A.; Tragni, M. Gold Catalyzed Direct Activation of Allylic Alcohols in the Stereoselective Synthesis of Functionalized 2-Vinyl-Morpholines. *Chem. Eur. J.* **2010**, *16*, 14272–14277.
(39) Cera, G.; Crispino, P.; Monari, M.; Bandini, M. Stereoselective Synthesis of Tetracyclic Indolines via Gold-Catalyzed Cascade Cyclization Reactions. *Chem. Commun.* **2011**, *47*, 7803–7805.
(40) Cera, G.; Chiarucci, M.; Mazzanti, A.; Mancinelli, M.; Bandini, M. Enantioselective Gold-Catalyzed Synthesis of Polycyclic Indolines. *Org. Lett.* **2012**, *14*, 1350–1353.
(41) Chiarucci, M.; di Lillo, M.; Romaniello, A.; Cozzi, P. G.; Cera, G.; Bandini, M. Gold Meets Enamine Catalysis in the Enantioselective alpha-Allylic Alkylation of Aldehydes with Alcohols. *Chem. Sci.* **2012**, *2*, 2859–2863.
(42) Bandini, M.; Bottoni, A.; Chiarucci, M.; Cera, G.; Miscione, G. P. Mechanistic Insights into Enantioselective Gold-Catalyzed Allylation of Indoles with Alcohols: the Counterion Effect. *J. Am. Chem. Soc.* **2012**, *134*, 20690–20700.
(43) Chiarucci, M.; Mocci, R.; Syntrivanis, L.-D.; Cera, G.; Mazzanti, A.; Bandini, M. Merging Synthesis and Enantioselective Functionalization of Indoles via Gold-catalyzed Asymmetric Cascade Reaction. *Angew. Chem., Int. Ed.* **2013**, *52*, 10850–10853.
(44) An, J.; Parodi, A.; Monari, M.; Reis, M. C.; Lopez, C. S.; Bandini, M. Gold-Catalyzed Dearomatization of 2-Naphthols with Alkynes. *Chem. Eur. J.* **2017**, *23*, 2442–2449.
(45) Cid, M. M.; Lago-Silva, M.; Gonzalez Comesaña, M.; Nieto Faza, O.; Silva Lopez, C. Computational and Experimental Studies on Cu/Au-catalyzed Stereoselective Synthesis of 1,3-disubstituted Allenes. *Org. Chem. Front.* **2019**, *6*, 1780–1786.
(46) Pedrazzani, R.; Pinosa, E.; Bertuzzi, B.; Monari, M.; Lauzon, S.; Ollevier, T.; Bandini, M. Convenient Synthesis of Polycyclic N(1)-C(2)-Fused Oxazino-indolones via [Au(I)] Catalyzed Hydrocarboxylation of Allenes. *Chem. Commun.* **2022**, *58*, 8698–8701.
(47) Pedrazzani, R.; Pintus, A.; De Ventura, R.; Marchini, M.; Ceroni, P.; Silva López, C.; Monari, M.; Bandini, M. New Fine-Tunable P_n/T_n-ImPy Gold Complexes: Synthesis, Characterization and Application in Dearomatization Reactions. *ACS Org. Inorg. Au* **2022**, *2*, 229–235.
(48) Pedrazzani, R.; Kiriakidi, S.; Monari, M.; Lazzarini, I.; Bertuzzi, G.; Silva López, C.; Bandini, M. Fluorinated Biphenyl Phosphine Ligands for Accelerated [Au(I)]-Catalysis. *ACS Catal.* **2024**, *14*, 6128–6136.
(49) Giovanelli, R.; Gallorini, G.; Huang, Y.; Brunetti, A.; Nikopoulos, K. D.; Monari, M.; Silva López, C.; Kiriakidi, S.; Bertuzzi, G.; Bandini, M. Dual [Au(I)]-Catalysis in Regioselective Cycloaddition of Bicyclo[1.1.0]butanes with Allene. *ACS Catal.* **2025**, *15*, 15698–15705.
(50) Hu, F.; Zhao, Y.; Che, L.; Yan, X.; Xia, Y. Recent Advances in Asymmetric Synthesis of Chiral Cyclobutenes. *ChemCatChem* **2024**, *16*, No. e202301249.
(51) Lu, R.; Yang, J.; Jiang, J.-M.; Wang, J.; Huang, W.; Peng, C.; Zhan, G.; Han, B. Catalyst-Controlled Divergent Synthesis of Bicyclo[2.1.1]hexanes and Cyclobutenes: The Unique Effect of Au(I). *JACS Au* **2025**, *5*, 2738–2748.
(52) Mato, M.; Franchino, A.; García-Morales, C.; Echavarren, A. M. Gold-Catalyzed Synthesis of Small Rings. *Chem. Rev.* **2021**, *121*, 8613–8684.
(53) Wu, H.; Zi, W.; Li, G.; Lu, H.; Toste, F.D. Gold(I)-Catalyzed Desymmetrization of 1,4-Dienes by an Enantioselective Tandem Alkoxylation/Claisen Rearrangement. *Angew. Chem., Int. Ed.* **2015**, *54*, 8529–8532.
(54) Zi, W.; Toste, F. D. Gold(I)-Catalyzed Enantioselective Desymmetrization of 1,3-Diols through Intramolecular Hydroalkoxylation of Allenes. *Angew. Chem., Int. Ed.* **2015**, *54*, 14447–14451.
(55) Sota, Y.; Yamamoto, M.; Murai, M.; Uenishi, J.; Uemura, M. Gold(I)-Catalyed Asymmetric Desymmetrization of *meso*-Alkynyl Diols and Kinetic Resolutions of the Corresponding DL-Diols: Effects of Celite Filtration and Silver Salts. *Chem. Eur. J.* **2015**, *21*, 4398–4404.
(56) Zheng, Y.; Guo, L.; Zi, W. Enantioselective and Regioselective Hydroetherification of Alkynes by Gold-Catalyzed Desymmetrization of Prochiral Phenols with P-Stereogenic Centers. *Org. Lett.* **2018**, *20*, 7039–7043.
(57) Lin, B.; Yang, T.; Zhang, D.; Zhou, Y.; Wu, L.; Qiu, J.; Chen, G.-Q.; Che, C.-M.; Zhang, X. Gold-Catalyzed Desymmetric Lactonization of Alkynylmalonic Acids Enabled by Chiral Bifunctional P,N ligands. *Angew. Chem., Int. Ed.* **2022**, *61*, No. e202201739.
(58) Kohnke, P.; Zhang, L. Gold(I)-Catalyzed Desymmetrization of Homopropargylic Alcohols via Cycloisomerization: Enantioselective Synthesis of Cyclopentenes Featuring a Quaternary Chiral Center. *Angew. Chem., Int. Ed.* **2024**, *63*, No. e202411292.
(59) Hashmi, A. S. K. Dual Gold Catalysis. *Acc. Chem. Res.* **2014**, *47*, 864–876.
(60) Zhao, X.; Rudolph, M.; Hashmi, A. S. K. Dual Gold Catalysis – an Update. *Chem. Commun.* **2019**, *55*, 12127–12135.
(61) Wang, W.; Ji, C. L.; Liu, K.; Zhao, C. G.; Li, W.; Xie, J. Dinuclear Gold Catalysis. *Chem. Soc. Rev.* **2021**, *50*, 1874–1912.
(62) Romano, C.; Jia, M.; Monari, M.; Manoni, E.; Bandini, M. Metal-free Enantioselective Electrophilic Activation of Allenamides: Stereoselective De-aromatization of Indoles. *Angew. Chem., Int. Ed.* **2014**, *53*, 13854–13857.
(63) Jia, M.; Monari, M.; Yang, Q. Q.; Bandini, M. Enantioselective Gold Catalyzed Dearomative [2+2]-Cycloaddition between Indoles and Allenamides. *Chem. Commun.* **2015**, *51*, 2320–2323.
(64) Rocchigiani, L.; Jia, M.; Bandini, M.; Macchioni, A. Assessing the Role of Counterion in Gold Catalyzed Dearomatization of Indoles with Allenamides by NMR Studies. *ACS Catal.* **2015**, *5*, 3911–3915.

https://doi.org/10.1021/acscatal.6c02231
ACS Catal. 2026, 16, 10721–10729

(65) Ocello, R.; De Nisi, A.; Jia, M.; Yang, Q.; Monari, M.; Giacinto, P.; Bottoni, A.; Miscione, G. P.; Bandini, M. Gold(I)-Catalyzed Dearomative [2+2]-Cycloaddition of Indoles with Activated Allenes: A Combined Experimental−Computational Study. *Chem. − Eur. J.* **2015**, *21*, 18445–18453.
(66) Lemos, B. C.; Venturini Filho, E.; Fiorot, R. G.; Medici, F.; Greco, S. J.; Benaglia, M. Enantioselective Povarov reactions: An update of a Powerful Catalytic Synthetic Methodology. *Eur. J. Org. Chem.* **2022**, *2022*, No. e202101171.
(67) Ferreira de Paiva, W.; de Freitas Rego, Y.; de Fátima, Â. The Povarov Reaction: A Versatile Method to Synthesize Tetrahydroquinolines, Quinolines and Julolidines. *Synthesis* **2022**, *54*, 3162–3179.
(68) Stevanović, D.; Bertuzzi, G.; Mazzanti, A.; Fochi, M.; Bernardi, L. Catalytic Enantioselective Povarov Reactions of Ferrocenecarbaldehyde-Derived Imines − Brønsted Acid Catalysis at Parts-Per-Million Level Loading. *Adv. Synth. Catal.* **2018**, *360*, 893–900.
(69) Bisag, G. D.; Pecorari, D.; Mazzanti, A.; Bernardi, L.; Fochi, M.; Bencivenni, G.; Bertuzzi, G.; Corti, V. Central-to-Axial Chirality Conversion Approach Designed on Organocatalytic Enantioselective Povarov Cycloadditions: First Access to Configurationally Stable Indole−Quinoline Atropisomers. *Chem. − Eur. J.* **2019**, *25*, 15694–15701.
(70) Satyanarayana, T.; Abraham, S.; Kagan, H. B. Nonlinear Effects in Asymmetric Catalysis. *Angew. Chem., Int. Ed.* **2008**, *48*, 456–494.
(71) Geiger, Y.; Bellemin-Laponnaz, S. Non-Linear Effects in Asymmetric Catalysis: Impact of Catalyst Precipitation. *ChemCatChem* **2022**, *14*, No. e202200165.
(72) Simmons, E. M.; Hartwig, J. F. On the Interpretation of Deuterium Kinetic Isotope Effects in C−H Bond Functionalizations by Transition-Metal Complexes. *Angew. Chem., Int. Ed.* **2012**, *51*, 3066–3072.
(73) Brandenburg, J.-G.; Bannwarth, C.; Hansen, A.; Grimme, S. B97-3c: A Revised Low-Cost Variant of the B97-D Density Functional Method. *J. Chem. Phys.* **2018**, *148*, No. 064104.
(74) Neese, F. Software Update: The ORCA Program System—Version 6.0. *Wiley Interdiscip. Rev.: Comput. Mol. Sci.* **2025**, *15*, No. e70019.

https://doi.org/10.1021/acscatal.6c02231
ACS Catal. 2026, 16, 10721−10729